



## Analyzing redox balance in a synthetic yeast platform to improve utilization of brown macroalgae as feedstock

C.A. Contador<sup>a,b</sup>, C. Shene<sup>a,c</sup>, A. Olivera<sup>a,b</sup>, Y. Yoshikuni<sup>d</sup>, A. Buschmann<sup>a,e</sup>,  
B.A. Andrews<sup>a,b</sup>, J.A. Asenjo<sup>a,b,\*</sup>

<sup>a</sup> Centre for Biotechnology and Bioengineering, CeBiB, Chile

<sup>b</sup> Department of Chemical Engineering and Biotechnology, University of Chile, Beauchef 850, Santiago, Chile

<sup>c</sup> Department of Chemical Engineering, University of La Frontera, Temuco, Chile

<sup>d</sup> Bio Architecture Lab, USA

<sup>e</sup> Consorcio BALBiofuel, Camino Chiquihue km6, Puerto Montt, Chile and Centro i-mar, Universidad de Los Lagos, Puerto Montt, Chile

### ARTICLE INFO

#### Article history:

Received 9 April 2015

Accepted 19 June 2015

Available online 10 July 2015

#### Keywords:

*Saccharomyces cerevisiae*

Biofuels

Brown macroalgae

Genome-scale model

Redox metabolism

Alginate

### ABSTRACT

Macroalgae have high potential to be an efficient, and sustainable feedstock for the production of biofuels and other more valuable chemicals. Attempts have been made to enable the co-fermentation of alginate and mannitol by *Saccharomyces cerevisiae* to unlock the full potential of this marine biomass. However, the efficient use of the sugars derived from macroalgae depends on the equilibrium of cofactors derived from the alginate and mannitol catabolic pathways. There are a number of strong metabolic limitations that have to be tackled before this bioconversion can be carried out efficiently by engineered yeast cells.

An analysis of the redox balance during ethanol fermentation from alginate and mannitol by *Saccharomyces cerevisiae* using metabolic engineering tools was carried out. To represent the strain designed for conversion of macroalgae carbohydrates to ethanol, a context-specific model was derived from the available yeast genome-scale metabolic reconstructions. Flux balance analysis and dynamic simulations were used to determine the flux distributions. The model indicates that ethanol production is determined by the activity of 4-deoxy-l-erythro-5-hexoseulose uronate (DEHU) reductase (DehR) and its preferences for NADH or NADPH which influences strongly the flow of cellular resources. Different scenarios were explored to determine the equilibrium between NAD(H) and NADP(H) that will lead to increased ethanol yields on mannitol and DEHU under anaerobic conditions. When rates of mannitol dehydrogenase and DehR<sub>NADH</sub> tend to be close to a ratio in the range 1–1.6, high growth rates and ethanol yields were predicted. The analysis shows a number of metabolic limitations that are not easily identified through experimental procedures such as quantifying the impact of the cofactor preference by DEHU reductase in the system, the low flux into the alginate catabolic pathway, and a detailed analysis of the redox balance. These results show that production of ethanol and other chemicals can be optimized if a redox balance is achieved. A possible methodology to achieve this balance is presented. This paper shows how metabolic engineering tools are essential to comprehend and overcome this limitation.

© 2015 The Authors. Published by Elsevier B.V. International Metabolic Engineering Society. This is an open access article under the CC BY-NC-ND license (<http://creativecommons.org/licenses/by-nc-nd/4.0/>).

### 1. Introduction

Depletion of fossil resources, increasing demand for fuel and climate change have encouraged the use of more efficient and sustainable sources to produce valuable products and energy (Jang et al., 2012). Microbial fermentation of biomass from diverse sources has been used to overcome this challenge. Corn and sugarcane biomass have been successfully used to produce biofuels

\* Corresponding author at: Centre for Biotechnology and Bioengineering, CeBiB, Chile. Fax: 56 22 6991084.

E-mail address: [juasenjo@ing.uchile.cl](mailto:juasenjo@ing.uchile.cl) (J.A. Asenjo).

<http://dx.doi.org/10.1016/j.meten.2015.06.004>

2214-0301/© 2015 The Authors. Published by Elsevier B.V. International Metabolic Engineering Society. This is an open access article under the CC BY-NC-ND license (<http://creativecommons.org/licenses/by-nc-nd/4.0/>).

at high yields using well-established fermentation technology, but their long-term use is questionable due to the competition between fuel and food resources. Although lignocellulosic plant materials are an alternative, the process and related costs to release sugars are extremely high and complex. In the past years, macroalgae, so-called seaweeds, have attracted attention for their high potential as feedstock to produce sustainable biofuels and commodity chemical compounds. Brown macroalgae has several key features: (1) its cultivation does not impact food supplies since it does not require fresh water resources or arable land; (2) brown macroalgae do not contain lignin which implies that its cell wall is structurally flexible; and (3) macroalgae are already being mass-cultivated in several countries (Jung et al., 2013).

The major polysaccharide constituent of brown macroalgae is alginate (30–60% of the total carbohydrates). Alginate is composed of  $\beta$ -D-mannuronate (M) and  $\alpha$ -L-guluronate (G) which are linked by 1,4-glycosidic bonds. These uronic acids can be arranged as M-blocks, G-blocks and alternative blocks of M and G units (Rehm, 2009). Mannitol and glucan (present as laminarin and cellulose) complete the carbohydrate composition. A key criterion for the economic and efficient use of the various sugars derived from brown macroalgae implies identification or design of microorganisms that can metabolize these carbohydrates. Metabolic engineering and genetic transformation play an important role to improve product yields and in the efficient use of this biomass. At present, many efforts are being made to engineer well-characterized microorganisms to utilize alginate and mannitol as carbon sources (Enquist-Newman et al., 2014; Wargacki et al., 2012). Enquist-Newman et al. (2014) have shown that ethanol can be produced from the co-fermentation of mannitol and an alginate monomer (4-deoxy-L-erythro-5-hexoseulose uronate, or DEHU) by *Saccharomyces cerevisiae*. They circumvent the limitations of the native strain by engineering both the mannitol and alginate catabolic pathways (Enquist-Newman et al., 2014). The native mannitol metabolic pathway was deregulated. The *Vibrio splendidus* alginate metabolism pathway was reconstructed in yeast together with the integration of the DEHU transporter of *Asteromyces cruciatis*. The efficiency of the mannitol and alginate metabolism pathways to produce ethanol depends on the redox control. Mannitol as a polyol generates excess reducing equivalents which must be redox balanced through an electron shunt. For ethanol production, alginate metabolism provides a counter balance to consume two reducing equivalents per mole of alginate. This electron transfer enabled ethanol fermentation from these sugars. Thus, a key step in this specific design was the selection of a DEHU reductase (DehR) with optimal cofactor preference for redox-balance, it preferentially uses NADH and co-uses NADH and NADPH. Fig. 1 describes the cofactor balance to generate ethanol in the engineered *S. cerevisiae*.

Ethanol fermentation from mannitol and DEHU was achieved under two specific growth conditions, 1:2 M ratio of DEHU:mannitol at 6.5% (w/v) and 9.8% (w/v) total sugars where the ratios of mannitol:DEHU consumptions were 2.4 and 2.1, respectively. In

both cases, glycerol is the main by-product as it helps to achieve a cofactor balance. However, no other ratios of mannitol:DEHU uptakes were reported. In addition, metabolism of DEHU could lead to a deficit of NADH. Yeast needs an excess of NADH to generate ethanol. In order to increase the bioconversion to ethanol from brown macroalgae sugars and allow biomass formation and metabolic maintenance, it is necessary to quantify the ability of DehR for co-use of NADH and NADPH and its impact on the redox balance and ethanol production under different ratio consumption rates. In this study, we aim to identify the optimal flux distribution through DehR to decrease by-products and increase the ethanol yield on alginate and mannitol. To represent the engineered strain used for bioconversion of brown macroalgae sugars to ethanol, we used a context-specific model derived from the most updated yeast genome-scale metabolic reconstruction (Heavner et al., 2012). We evaluated the network by comparing *in silico* biomass formation and by-production rates to *in vivo* measurements. Flux balance analysis was used for *in silico* characterization of the current metabolic state of the yeast platform and the strategies proposed to achieve the optimal distribution (Orth et al., 2010).

## 2. Methodology

### 2.1. Metabolic model

To mimic the cellular behaviour of the synthetic yeast platform for bioconversion of brown macroalgae sugars to ethanol a previously described genome-scale model was used to represent *S. cerevisiae* metabolism. This corresponds to an updated version of Yeast5 (Heavner et al., 2012). The yeast systems biology community carried out this reconstruction and it includes 910 genes, 3490 reactions and 2220 metabolites. The network is fully compartmentalized, elementally-balanced and no regulatory constraints have been included yet. The reconstruction is available at <http://www.comp-sys-bio.org/yeastnet/>.

The biochemical reactions of the reconstruction define a stoichiometric matrix that allows testing of the capabilities of the system based on structural knowledge of the metabolic reaction network and steady-state flux distributions. The stoichiometry-

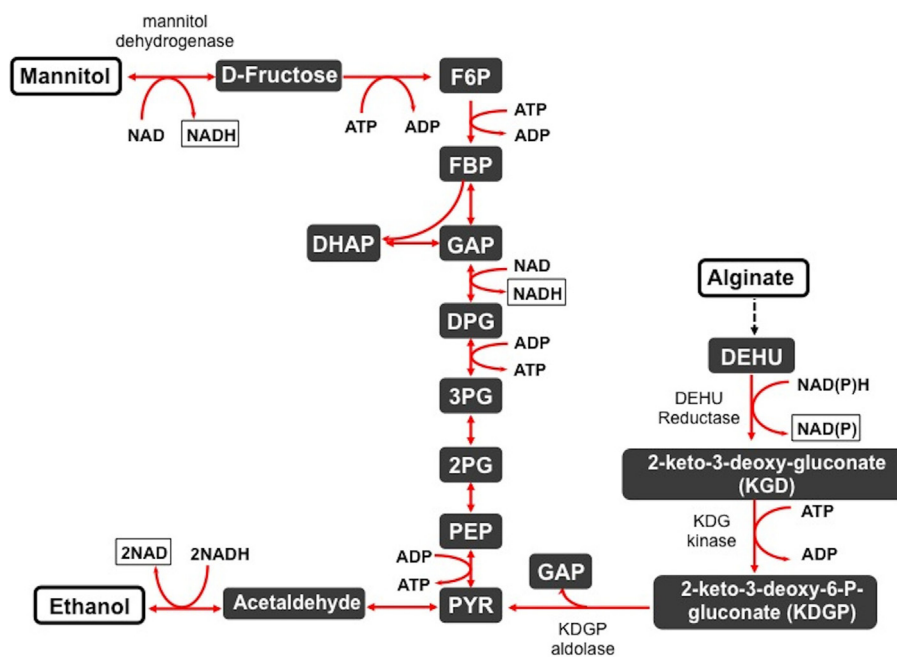


Fig. 1. Overview of cofactor requirements in the engineered *S. cerevisiae* strain.

oriented approaches are based on a material balance of each metabolite using a quasi-steady state approximation (Llaneras and Pico, 2008; Savinell and Palsson, 1992; Varma and Palsson, 1994):

$$S \cdot \mathbf{v} = 0 \quad (1)$$

where  $S$  is the  $m \times n$  stoichiometric matrix consisting of  $m$  metabolites and  $n$  net reactions, and  $\mathbf{v}$  is the  $n \times 1$  vector of net reaction rates. Constraint-based linear optimization was applied to calculate the optimal production flux distributions under specific conditions (Becker et al., 2007; Schellenberger et al., 2011). This method utilizes linear optimization to estimate optimum values one can achieve given a particular objective function  $Z$ .

## 2.2. In silico strain

*S. cerevisiae* can use different sugars to grow. However, alginate is not a natural carbon source for yeast. In addition, only some strains of *S. cerevisiae* are able to assimilate mannitol whose transport and metabolism is not fully understood (Maxwell and Edward, 1971; Quain and Boulton, 1987). Therefore, the reconstruction of *S. cerevisiae* does not include pathways related to the assimilation of alginate and mannitol. These pathways must be added to simulate the use of brown macroalgae sugars for ethanol production by yeast. In addition, the co-use of NADH and NADPH by DehR was incorporated into the reconstruction. Following are the reactions added to represent the synthetic yeast platform:

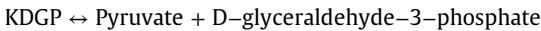
(i) DEHU reductase (DehR), both NADH and NADPH-dependent



(ii) KDG kinase



(iii) KDGP aldolase



(iv) Mannitol dehydrogenase



Exchange and transport reactions were added for both carbon sources.

According to the strain's genetic background, the SUC2 gene (YIL162W), which encodes two different forms of invertase, is deleted (Enquist-Newman et al., 2014). Therefore, SUC2 gene was deleted to simulate the genetic background of the strain.

## 2.3. In silico growth conditions

Simulations were performed for anaerobic growth on High-Carbon (HC) media with alginate and mannitol as the carbon sources (Enquist-Newman et al., 2014). HC medium contains vitamins, trace elements, minerals and a mix of amino acids and adenine as nitrogen sources. Details of media composition have been described by Enquist-Newman et al. (2014). The uptake rates of vitamins and amino acids were set to 10 and 1 mmol g DW<sup>-1</sup> h<sup>-1</sup>, respectively (Mo et al., 2009). Trace elements and minerals were assumed to be non-limiting. Ergosterol and unsaturated fatty acids were set at non-limiting but low levels. Sterols and unsaturated fatty acids are required for optimal growth of *S. cerevisiae* under strictly anaerobic conditions (Schulze, 1995). The anaerobic condition was modeled by assuming an oxygen uptake rate equal to zero. With the objective to include aspects of the anaerobic physiology of *S. cerevisiae*, new constraints were added to simulate growth under anaerobic conditions as yeast

responds differently to aerobic or anaerobic environments. It has been observed that during anaerobic fermentation the TCA cycle splits into two separate branches, an oxidative and a reductive branch (Nissen et al., 1997). Therefore, the TCA cycle was forced to act as two branches. This was achieved by bounding to zero the reactions associated to succinate dehydrogenase and succinyl-CoA ligase genes. From literature other constraints have been proposed such as bounding to zero the quinone-mediated reactions involving FADH<sub>2</sub> and NADH reoxidation (Vargas et al., 2011). The flux of non-growth associated ATP maintenance (ATPM) was fixed at 1 mmol g DW<sup>-1</sup> h<sup>-1</sup> (Mo et al., 2009). This reaction simulates the consumption of ATP by non-growth associated processes such as maintenance of electrochemical gradients.

## 2.4. In silico predictions on mannitol and DEHU mixtures

To generate predictions consistent with the experimental data under anaerobic conditions, the specific mannitol uptake rate (MUR) and acetate formation rate (AFR) were determined from the data points presented by Enquist-Newman et al. (2014) after spline smoothing. This procedure was done for the two growth conditions, renamed scenario 1 and 2, in which a ratio of mannitol:DEHU consumption of 2.4 and 2.1 were assumed respectively. The MUR and AFR (g g DW<sup>-1</sup> h<sup>-1</sup>) were modeled as

Scenario 1

$$\text{MUR} = \frac{0.39M}{4.31 + M + D + \frac{E^2}{28.7}} \quad (2)$$

$$\text{AFR} = \frac{4.6 \cdot 10^{-4}M}{1 + 0.108D} \quad (3)$$

Scenario 2

$$\text{MUR} = \frac{0.373M}{18.77 + M + D + \frac{E^2}{6.89}} \quad (4)$$

$$\text{AFR} = 7.9 \cdot 10^{-7}M + 4.4 \cdot 10^{-4}D \quad (5)$$

where  $M$ ,  $D$ , and  $E$  are mannitol, DEHU and ethanol concentrations (g/L), respectively. Initial concentrations were used to calculate MUR by Eqs. (2) and (4). DEHU uptake rates (DUR) were determined by the sugar consumption ratios and MUR. These rates were used as constraints in the simulations.

To simulate the time course profiles described in the literature (Enquist-Newman et al., 2014), a bi-level optimization problem was formulated to calculate the specific growth rates ( $\mu$ ) and specific production rates:

Maximize  $Z = v_{\text{ethanol}}$   
 subject to  
 maximize  $\mu$   
 subject to

$$\sum_j S_{ij} v_j = 0 \quad \forall i \in M$$

$$v_{\text{DEHU}} = \frac{v_{\text{mannitol}}}{\text{ratio}}$$

$$v_{\text{ATPM}} = v_{\text{maintenance}}$$

$$v_{\text{oxygen}} = 0$$

$$v_{j,\text{rev}} \in R$$

$$v_{j,\text{irrev}} \in R_0^+$$

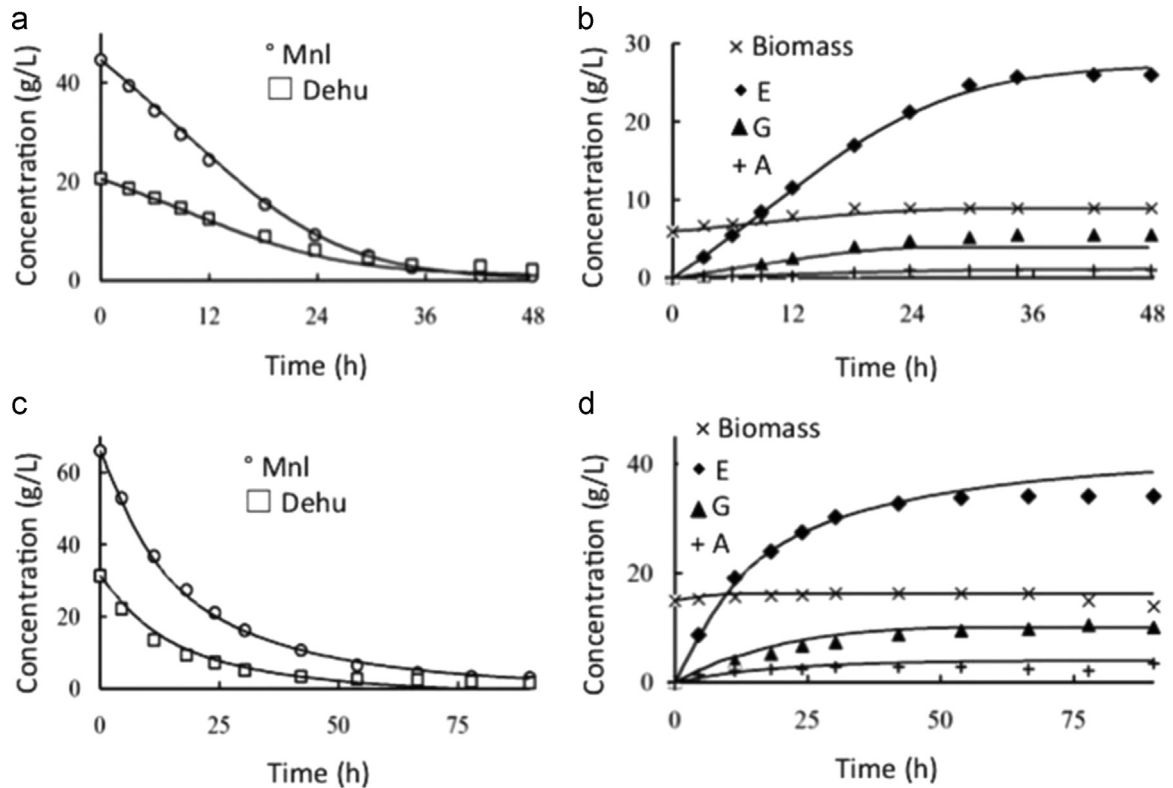


**Fig. 2.** Simulation of ethanol fermentation from mannitol and DEHU. Growth rates (B) and secretion profiles for ethanol (E), glycerol (G) and acetate (A) were calculated for scenario 1 (a,b) and scenario 2 (c,d) assuming a ratio of mannitol:DEHU consumption of 2.4 and 2.1, respectively. Experimental data is represented by symbols, and continuous lines represent simulated values.

where  $v_{DEHU}$ ,  $v_{mannitol}$ ,  $v_{oxygen}$ ,  $v_{ethanol}$  and  $v_{ATPM}$  correspond to DEHU, mannitol and oxygen uptake rates, ethanol production rate and non-growth associated ATP for maintenance (ATPM), respectively. MUR and AFR at each time point were used as inputs to calculate the pseudo-steady-states. To simulate the late growth phase time points,  $\mu$  was bound to zero and then ethanol production rate was maximized adding as constraint the minimization of ATP consumption for maintenance. These assumptions were deemed reasonable due to the depletion of essential nutrients and carbon sources. In several studies maintenance of energy requirements have been reported at values lower than  $1 \text{ mmol g DW}^{-1} \text{ h}^{-1}$  (Gustafsson et al., 1993). The calculated growth, uptake and production rates were used to determine biomass, substrate, and product concentrations at each time point as follows:

$$\frac{dC_j}{dt} = r_j \cdot C_x \quad (6)$$

where  $r_j$  is the substrate uptake rate or product formation rate,  $C_j$  the concentration of product/substrate and  $C_x$  the biomass concentration. It was assumed that the rates remain constant during each 0.5 h integration step. The solution to this equation was fitted to the experimental data. All simulations were performed using MATLAB and the COBRA Toolbox software packages with Gurobi™ Optimizer (Gurobi Optimization, Inc., Houston, TX) (Becker et al., 2007; Schellenberger et al., 2011).

### 3. Results and discussion

A genome-scale model of the *S. cerevisiae* metabolism (Heavner et al., 2012) was used to simulate and assess biomass and by-product formation in a strain designed for bioconversion of brown macroalgae sugars to ethanol. Two conditions defined by the ratio

of mannitol:DEHU consumption, 2.4 and 2.1 at 6.5% (w/v) and 9.8% (w/v) total sugars respectively, were evaluated experimentally under anaerobic and microaerobic conditions to gain insight into the metabolic behavior of this strain. Experimental data points were present by Enquist-Newman et al. (2014). In this study, this data was used to validate the model and to specify any model inconsistencies. The two conditions will be referred to as scenarios 1 and 2.

#### 3.1. Dynamic simulation of experimental data

Dynamic simulations of ethanol fermentation from mannitol and DEHU were performed to compare the simulated profiles with the published time course data (Enquist-Newman et al., 2014). From the initial simulations it was observed that the calculated specific growth rates under anaerobic conditions were too low to achieve the experimental biomass concentrations. According to Enquist-Newman et al. (2014), the strains developed were unable to grow anaerobically in liquid culture, thus strains were adapted and selected on agar plates with HC media containing DEHU and mannitol. Actively growing aerobic cells were used as inoculum. On the other hand, it has been mentioned that direct measurement of low concentrations of oxygen, such as the oxygen probe and redox potential, only indicate the activity of the oxygen in the medium, but do not provide information of the oxygen flux (Visser et al., 1990). Thus, traces of oxygen may be available and explain the difference between the model estimations and experimental data since only extracellular measurements are available.

Limited oxygen levels were analyzed and additional constraints were added to the genome-scale model to simulate and fit the time course profiles (Hjersted et al., 2007). Oxygen uptake rate was set in dynamic simulations to minimize the difference between the experimental and predicted biomass concentration. In

this way, traces of oxygen and strictly anaerobic growth can be simulated. In addition, it was assumed that only the by-products reported as synthesized by the strain are being produced. Fig. 2 shows the simulated scenarios against the time course profiles. A good fit is observed both for scenarios 1 and 2 where the model accurately predicts the transition between growth phases and by-product synthesis. Slight differences are observed for ethanol and glycerol curves in Fig. 2b and d. The additional constraints on oxygen are essential to mimic the metabolic behavior of the strain.

### 3.2. Effect of DehR cofactor use

As stated above, the engineered *S. cerevisiae* strain is able to metabolize alginate monomers, DEHU, through the expression of DehR which co-uses NADH and NADPH. However, it can be seen that even when the external fluxes are determined, there is an additional degree of freedom at the metabolite DEHU where the flux coming into the system is split between  $DehR_{NADH}$  and  $DehR_{NADPH}$ . A sensitivity analysis was done to evaluate the effect of the preference for a specific cofactor by DehR on the flux distributions that characterize the current metabolic states. For that purpose, different fractions of DEHU flux through the reactions catalyzed by DehR,  $DehR_{NADH}$  and  $DehR_{NADPH}$ , were evaluated. Five cases were evaluated for scenarios 1 and 2, respectively. Fractions were selected to range from 0 to 1 to consider cases where all the flux is directed to only one of the reactions catalyzed by DehR. The total flux through  $DehR_{NADH}$  and  $DehR_{NADPH}$  must be equal to DEHU uptake rate (DUR). The final concentrations of biomass, ethanol and glycerol were calculated as shown in Table 1. According to scenario 1, experimental values of biomass, ethanol and glycerol are 8.97, 26.19, and 5.5 g/L, respectively. In this case, it is observed that while biomass and ethanol concentrations are well represented by the model, glycerol concentrations have a lower production depending on the flux distribution through  $DehR_{NADH}$  and  $DehR_{NADPH}$ . The highest difference, 42%, was registered when all DEHU flux goes through  $DehR_{NADH}$ . This behavior is corrected as the flux through  $DehR_{NADPH}$  increases. In yeasts, glycerol is produced by the reduction of dihydroxyacetone phosphate (DHAP) to glycerol-3-phosphate (G3P), a reaction catalyzed by cytosolic NAD<sup>+</sup>-dependent G3P dehydrogenase; G3P is subsequently dephosphorylated by a glycerol-3-phosphatase. During anaerobic growth, glycerol production serves as a redox sink to maintain the cytosolic redox balance by consuming NADH (Overkamp et al., 2002). On the other hand, Table 1 shows that as the fraction of DEHU flux processed by  $DehR_{NADPH}$  increased, the OUR needed to attain the required biomass concentration also increased. It is also observed that ethanol production decreases although the difference is less than 10% compared to the experimental value. These results can be explained because of the role that NADP(H) plays in anabolism since many of the reactions involved in the biosynthesis

of amino acids, lipids and nucleotides use NADPH as the reducing agent. Due to the oxidation of NADPH by  $DehR_{NADPH}$ , less reducing agent is available to support the growth and thus more oxygen is needed. Additionally, the more NADH that goes to glycerol production, the less is available for ethanol production.

For scenario 2, experimental values of biomass, ethanol and glycerol are 16, 36.4, and 10.77 g/L, respectively. As in scenario 1, the biggest variations are for the calculated glycerol concentrations. As the fraction of DEHU flux processed by  $DehR_{NADPH}$  increased the OUR needed to attain the biomass concentration also increased and ethanol production decreases. However, in this case the best fit is obtained when 80% of DUR is processed through  $DehR_{NADH}$  and only 20% goes through  $DehR_{NADPH}$  where the OUR is almost zero. Differences in the flux distribution between scenarios are ascribed both to the different initial concentrations of biomass and the length of growth periods. In scenario 1, biomass concentration increased from 6 to 9 g/l in 18 h while in scenario 2, the increase was from 15 to 16 g/ in 30 h.

From these results, it is evident that DehR co-use of NADH and NADPH has an impact on ethanol production and by-product synthesis. To take a picture of the flux distribution and conditions that determine both scenarios, simulations were done at time 3 h where the cells are still growing. Fig. 3 shows the flux distributions obtained with the conditions of scenarios 1 and 2 at the mentioned time. In the first case, Fig. 3a, all DEHU is converted to 2-Keto-3-Deoxy-D-Gluconate (KDG) by the reaction  $DehR_{NADPH}$ . Consequently, the system must be adjusted to balance the reduced cofactor NADH produced in mannitol reduction. This is achieved through the synthesis of glycerol from DHAP. In addition, a fraction of DHAP is transported to the mitochondria where the NADH produced by malate dehydrogenase is used to produce G3P that is then transported to the cytosol. The glycerol produced reduces the excess of NADH in both the cytosol and mitochondria. On the other hand for scenario 2, Fig. 3b shows that DEHU is mostly oxidized through  $DehR_{NADH}$ , which contributes to oxidation of the NADH produced by mannitol reduction. In this case, the glycerol production rate is lower than in scenario 1. However, its production is still required to reduce the excess of NADH since the rate of the reaction catalyzed by mannitol dehydrogenase is higher than  $DehR_{NADH}$ . The lower growth rate implies that the rate of the reaction catalyzed by malate dehydrogenase is lower. In both cases, low growth rates are predicted to achieve the experimental values since cells seem to be at the end of the exponential phase.

### 3.3. Simulation of optimal ethanol production

In the experiments presented by Enquist-Newman et al. (2014), ethanol fermentations were performed from mannitol and DEHU at a specific molar ratio to mimic the sugars prepared via their biorefinery approach. However, macroalgae carbohydrate content varies depending on factors such as season and water depth (Adams et al., 2011; Draget et al., 2005) and even more important is the ratio of mannitol:DEHU consumption. Experimentally only two consumption ratios were presented, 2.4 and 2.1, that defined the two scenarios evaluated in this work. The energy and reducing agents generated by the system should be in proportion to the availability of carbon sources to generate biomass. If it is assumed that glucose is the optimum carbon source for yeast, the mannitol:DEHU ratio to produce the same amount of NADH and ATP than glucose is around 2. Thus, it could be of interest to analyze the system's response against changes in these variables and how ethanol production can be optimized. To study the influence of sugar consumption rate on cellular metabolism, mannitol uptake rate (MUR) was allowed to take values from 0.8 to 1.5 mmol g DW<sup>-1</sup> h<sup>-1</sup>. This interval covers experimental ranges and simulates new conditions since initial MUR were 1.38 and

**Table 1**  
Effect of DehR co-use of NADH and NADPH in the final concentrations of biomass, ethanol and glycerol (g/L) for scenarios 1 and 2. DEHU (DUR) and oxygen uptake rates (OUR) units are mmol g DW<sup>-1</sup> h<sup>-1</sup>.

Condition	$DehR_{NADH}$	Biomass	Ethanol	Glycerol	OUR
Scenario 1	DUR	9.0	26.8	3.2	0.06
	0.8DUR	9.0	26.1	3.3	0.10
	0.5DUR	9.0	25.2	4.2	0.14
	0.2DUR	9.0	24.5	4.8	0.19
	0	9.0	23.7	5.3	0.22
Scenario 2	DUR	16.3	39.1	6.3	0.01
	0.8DUR	16.3	38.4	9.1	0.01
	0.5DUR	16.3	36.5	8.0	0.05
	0.2DUR	16.3	33.7	7.7	0.10
	0	16.3	24.8	16.0	0.13

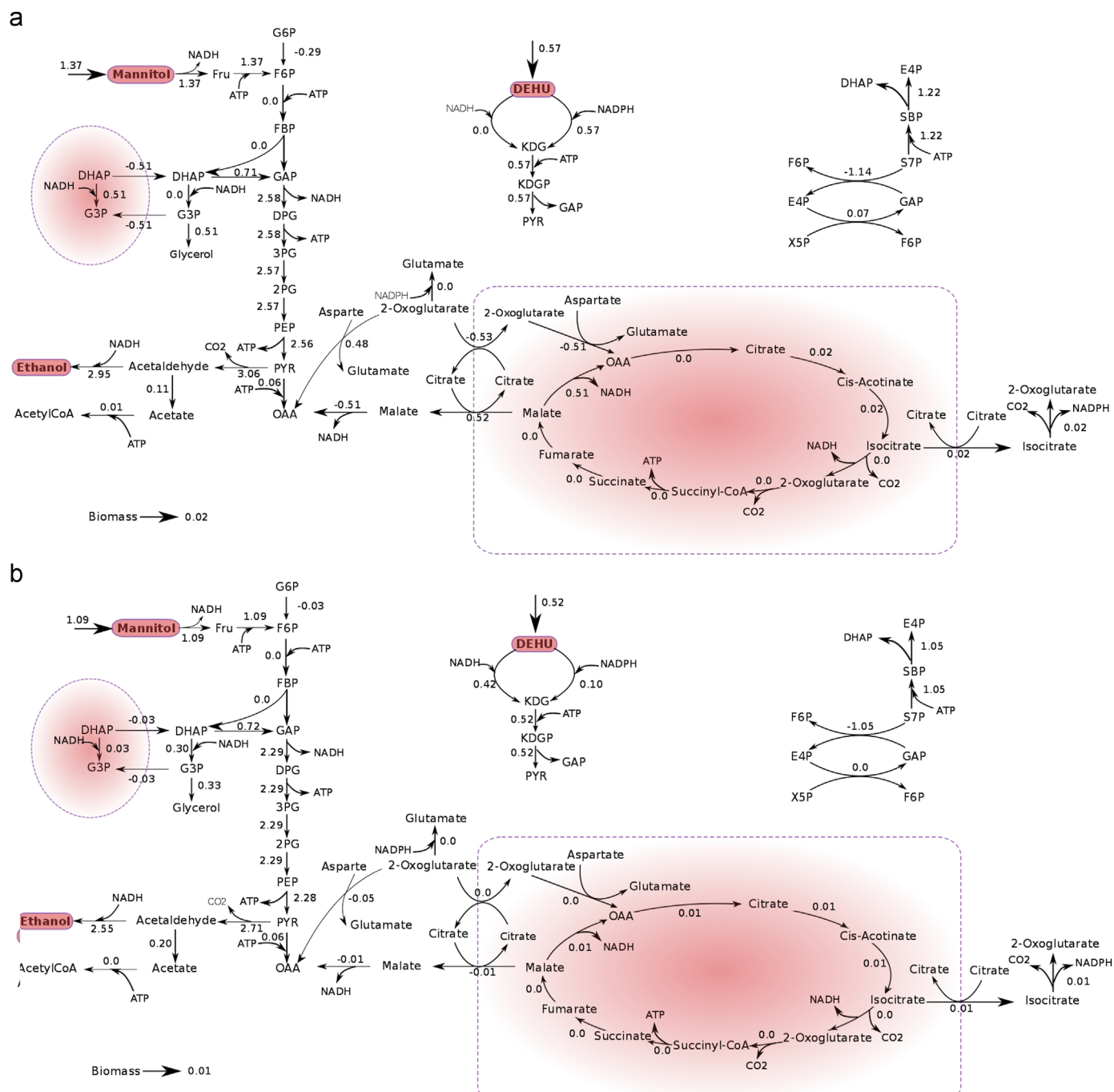


**Fig. 3.** Flux distributions at time 3 h: (a) Scenario 1 assuming  $DehR_{NADPH}=DUR$ , (b) Scenario 2 assuming  $DehR_{NADPH}=0.2DUR$ . All fluxes are in the direction of the arrows. A negative value means that the flux is in the direction opposite to the arrow.

$1.16 \text{ mmol g}^{-1} \text{ h}^{-1}$  for scenarios 1 and 2, respectively. The range for the ratio of mannitol:DEHU consumption was defined from 1 to 2.4. For the simulations, it was considered that the DEHU flux coming into the system is split into  $DehR_{NADH}$  and  $DehR_{NADPH}$ . Flux distributions were calculated assuming a split ratio of 80:20, respectively. This allows the co-use of NADH and NADPH with a preference for NADH. Simulations were also carried out assuming a split ratio of 96:4 where 96% of DEHU is processed by the NADH reductase. Results were extremely similar to those obtained with the 80:20 ratio which are explained in detail and shown in Fig. 4. This figure shows the effect of the ratio of mannitol:DEHU consumption and MUR over growth rate, ethanol, glycerol, and acetate production rates and substrate yield on ethanol. For the ranges

established, it is observed that the maximum growth rate,  $0.036 \text{ h}^{-1}$ , is achieved when MUR is in the region  $1.35\text{--}1.5 \text{ mmol g DW}^{-1} \text{ h}^{-1}$  and the ratio MUR:DUR is around 1, which means maximum growth is favored when both substrates are consumed at the same specific rates. In this case, the NADH produced in the reduction of mannitol is balanced through DEHU oxidation because a higher percentage of the DEHU flux goes through  $DehR_{NADH}$ . From Fig. 4a it can be observed that growth rate decreases as the mannitol uptake rate decreased and the ratio MUR:DUR increased. The initial growth rates for the MUR and ratio mannitol:DEHU experimental values registered for scenarios 1 and 2 are near the growth curves of 0.02 and  $0.015 \text{ h}^{-1}$ , respectively. These growth curves are away from the optimal growth

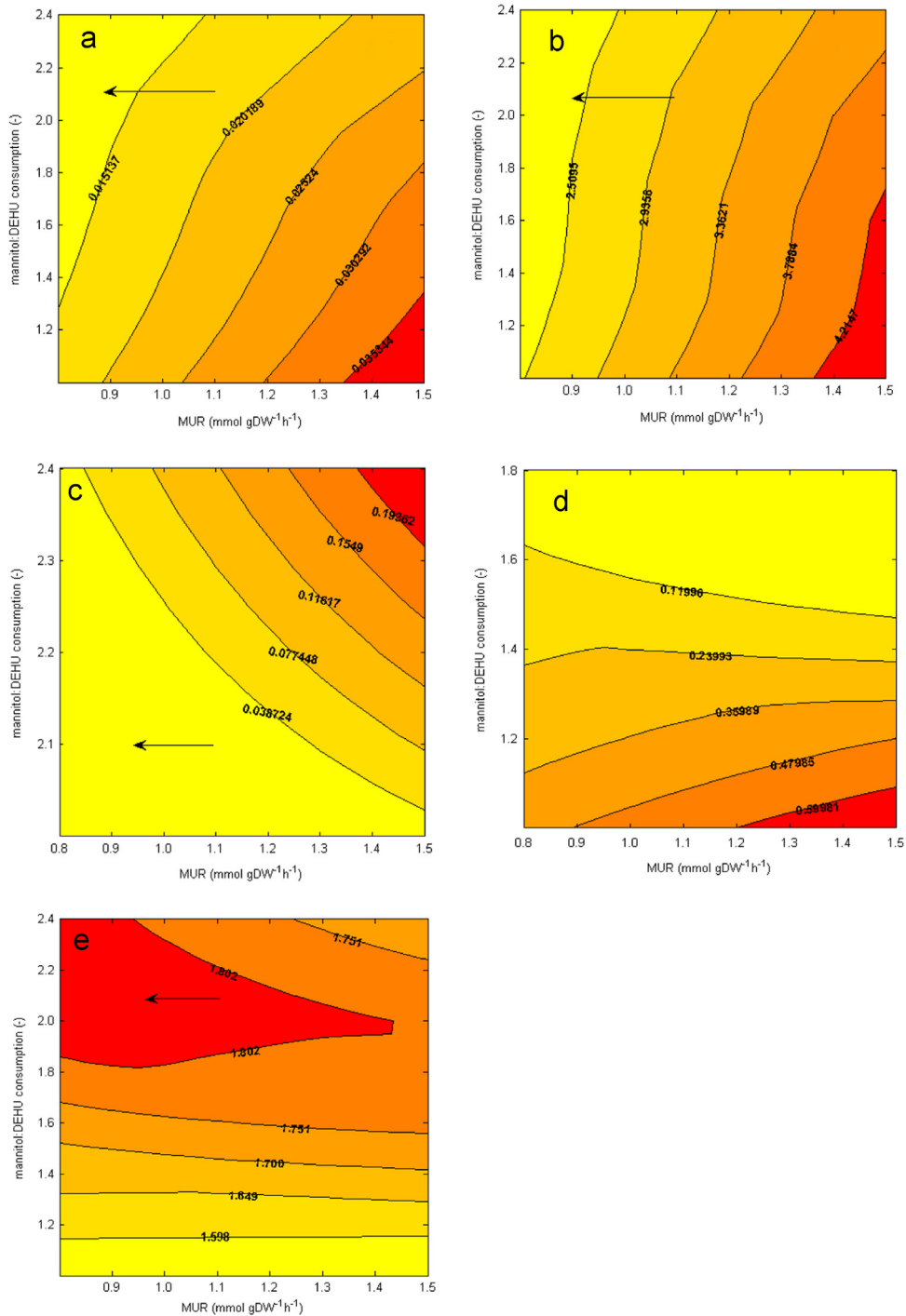


**Fig. 4.** Effect of the ratio of mannitol:DEHU consumption and mannitol uptake rates (MUR,  $\text{mmol g DW}^{-1} \text{h}^{-1}$ ) on (a) the specific growth rate ( $\text{h}^{-1}$ ), (b) ethanol, (c) glycerol and (d) acetate specific synthesis rates ( $\text{mmol g DW}^{-1} \text{h}^{-1}$ ), and (e) ethanol yield on substrate. The arrows show changes during growth under conditions of scenario 2 in batch fermentation.

conditions, which is important since ethanol production rates show a similar behavior to growth. Fig. 4b shows that ethanol production increases as the MUR increased and the ratio MUR: DUR decreased. The maximum ethanol production curve is reached when MUR is in the region  $1.35\text{--}1.5 \text{ mmol g DW}^{-1} \text{h}^{-1}$  and the ratio MUR:DUR is lower than 1.6. The ethanol production predicted for conditions under scenarios 1 and 2 are near to the production curves of  $3.36$  and  $2.51 \text{ mmol g DW}^{-1} \text{h}^{-1}$ , respectively. These values are lower than the maximum calculated. It is interesting to highlight that the model only predicts glycerol production at ratios of MUR:DUR higher than 2, which is the

current metabolic state of this strain. Glycerol and acetate production curves are shown in Fig. 4c and d. Acetate production curves are only predicted at ratios of MUR:DUR lower than 1.6 (Fig. 4d), acetate increases as the MUR increased and the ratio of MUR:DUR decreased. This behavior is explained since the NADPH produced by biosynthetic reactions must be oxidized. In this case, predicted values are slightly different from experimental data since according to scenario 2, acetate should be produced at a ratio of MUR:DUR equal to 2.1. The difference is explained by the trace elements of oxygen that were set to  $0.1 \text{ mmol g DW}^{-1} \text{h}^{-1}$ , a higher value than the best fit in Table 1. Finally, substrate yield on

ethanol as a function of MUR and the ratio MUR:DUR is shown in Fig. 4e. The maximum ethanol yield corresponds to the curve defined by a mannitol uptake rate between 0.8 and 1.2 mmol g DW<sup>-1</sup> h<sup>-1</sup> and a ratio of mannitol:DEHU higher than 1.8. This state is characterized by the absence of glycerol and acetate production. The conditions of the experimental data are found in the upper right corner of the diagram and inside the area defined for the maximum ethanol yield curve, respectively. However, experimental conditions are not able to reach maximum yield, because of by-product production. In addition, MUR changes during the process due to the decrease in substrate concentration and the increase in ethanol concentration (relationships in Eqs. (2) and (4)). Assuming constant ratios of mannitol:DEHU consumption (Enquist-Newman et al., 2014), the changes in growth rate, ethanol, and glycerol production rates and substrate yield on ethanol, respectively in the batch fermentation for scenario 2 were represented by an horizontal line in Fig. 4.

The fact that experimental data is not near optimal conditions is due to the low flux into the alginate catabolic pathway in spite of the current metabolic structure. This could be ascribed to a slower rate of DEHU transport compared to mannitol uptake rate and/or regulatory elements that are not included in the model for identification. For example, codon optimization of KDG Kinase from *E. coli* has shown high expression of the protein in *S. cerevisiae*. However, low enzyme activity has been reported in yeast (Benisch and Boles, 2014). This enzyme contains an [4Fe4S] cluster (Gardner and Fridovich, 1991) which possibly is not recognized as apoprotein for [FeS] incorporation or is inactivated by reactive oxygen species (ROS) due to an insufficient repair mechanism in yeast (Benisch and Boles, 2014). Benisch and Boles (2014) tested diverse strategies to improve enzyme activity without positive results. The optimized strain described by Enquist-Newman et al. (2014) has a genome-integrated KDG Kinase gene from *E. coli*. These factors must be evaluated in order to test other strategies to reach the desirable scenario such as to replace native enzymatic reactions with heterologous enzymes that have specificity for the opposite cofactor for engineering of the redox metabolism in *S. cerevisiae* (King and Feist, 2013; Bro et al., 2006).

#### 4. Conclusions

In this study, a genome-scale model of *S. cerevisiae* metabolism (Heavner et al., 2012) was used to simulate and assess biomass and by-product formation in a strain designed for bioconversion of brown macroalgae sugars to ethanol. Two conditions defined by the ratio of mannitol:DEHU consumption, 2.4 and 2.1, were evaluated experimentally under anaerobic conditions to gain insight into the metabolic behavior of this strain. Experimental data points were taken from Enquist-Newman et al. (2014). In this study, the two conditions were referred to as scenarios 1 and 2, respectively. The model predicted with accuracy biomass and product formation in the yeast platform under anaerobic conditions for scenarios 1 and 2. Since the entire flux map is not known, as only the external fluxes have been measured, a variety of split ratios were examined between  $DehR_{NADH}$  and  $DehR_{NADPH}$ . This allows the characterization of the current metabolic state of the strain. It was observed that the flux split into  $DehR_{NADH}$  and  $DehR_{NADPH}$  determines the redox balance of the system, by-product formation and ethanol production. The model shows that traces of oxygen must be present in the system. From the experimental data and simulations, the main by-product was glycerol. Glycerol is produced to reduce the excess of NADH when the rate of the reaction catalyzed by mannitol dehydrogenase is higher than  $DehR_{NADH}$ . Glycerol formation is undesirable in the industrial production of ethanol from carbohydrate feedstocks. Some

strategies have been suggested for reducing glycerol production by *S. cerevisiae* during fermentation (Albers et al., 1996; Weusthuis et al., 1994). For the co-fermentation of mannitol and DEHU, oxygen could be controlled to balance any difference between mannitol reduction and DEHU oxidation; however at a large scale oxygen control may be not feasible.

To optimize the current metabolic state, a serie of simulations were done to study the effect of the ratio of mannitol:DEHU consumption and mannitol uptake rates assuming the co-use of NADH and NADPH by  $DehR$  with a preference for NADH. It was observed that the relationship between the ratio of mannitol:DEHU consumption and mannitol uptake rate could favor a decrease or increase in growth and product formation. The conditions for maximum ethanol production were established when MUR was in the region between 1.35 and 1.5 mmol g DW<sup>-1</sup> h<sup>-1</sup> and the ratio MUR:DUR was lower than 1.6. This state is characterized for high growth rates, no glycerol production, low acetate production, and high ethanol yields. In this case, NADH produced in the oxidation of mannitol is balanced through DEHU reduction because a higher percentage of the DEHU flux goes into  $DehR_{NADH}$ .

In this study, we have shown that the full potential of brown macroalgae as feedstocks for biofuel production and other more valuable chemicals depends on the equilibrium of cofactors derived from the alginate and mannitol catabolic pathways. The genome-scale model is a useful tool to evaluate theoretically different hypothesis about the metabolic behavior of this strain. The analysis shows a number of metabolic limitations that are not easily identified through experimental procedures such as quantifying the impact of the cofactor preference by DEHU reductase in the system, the low flux into the alginate catabolic pathway, and a detailed analysis of the redox balance. These modern metabolic modeling tools are very useful to aid the research and development necessary to produce ethanol and other metabolites from brown macroalgae. This is a first modeling approach to assess the co-fermentation of manitol and an alginate monomer (DEHU) by *Saccharomyces cerevisiae*.

#### Acknowledgements

We would like to thank BAL for the support of a postdoctoral fellow (C.A.C.) and the Conicyt Basal Centre Grant for the CeBiB (FB0001).

#### Appendix A. Supplementary material

Supplementary data associated with this article can be found in the online version at <http://dx.doi.org/10.1016/j.meteno.2015.06.004>.

#### References

- Adams, J.M.M., Toop, T.A., Donnison, I.S., Gallagher, J.A., 2011. Seasonal variation in *Laminaria digitata* and its impact on biochemical conversion routes to biofuels. *Bioresour. Technol.* 102, 9976–9984.
- Albers, E., Larsson, C., Lidén, G., Niklasson, C., Gustafsson, L., 1996. Influence of the nitrogen source on *Saccharomyces cerevisiae*. Anaerobic growth and product formation. *Appl. Environ. Microbiol.* 62, 3187–3195.
- Becker, S.A., Feist, A.M., Mo, M.L., Hannum, G., Palsson, B.Ø., Herrgard, M.J., 2007. Quantitative prediction of cellular metabolism with constraint-based models: the COBRA toolbox. *Nat. Protoc.* 2, 727–738.
- Benisch, F., Boles, E., 2014. The bacterial Entner–Doudoroff pathway does not replace glycolysis in *Saccharomyces cerevisiae* due to the lack of activity of iron-sulfur cluster enzyme 6-phosphogluconate dehydratase. *J. Biotechnol.* 171, 45–55.
- Bro, C., Regenber, B., Förster, J., Nielsen, J., 2006. In silico aided metabolic engineering of *Saccharomyces cerevisiae* for improved bioethanol production.

- Metab. Eng. 8, 102–111.
- Draget, K.I., Smidsrød, O., Skjåk-brøn, G., 2005. Alginates from algae. In: Alexander Steinbüchel, Sang Ki Rhee (Eds). *Polysaccharides and Polyamides in the Food Industry*. Wiley-VCH Verlag GmbH & Co. KGaA, pp. 1–30.
- Enquist-Newman, M., Faust, A.M.E., Bravo, D.D., Santos, C.N.S., Raisner, R.M., Hanel, A., Sarvabhowman, P., Le, C., Regitsky, D.D., Cooper, S.R., Peereboom, L., Clark, A., Martinez, Y., Goldsmith, J., Cho, M.Y., Donohoue, P.D., Luo, L., Lamberson, B., Tamrakar, P., Kim, E.J., Villari, J.L., Gill, A., Tripathi, S.A., Karamchedu, P., Paredes, C.J., Rajgarhia, V., Kotlar, H.K., Bailey, R.B., Miller, D.J., Ohler, N.L., Swimmer, C., Yoshikuni, Y., 2014. Efficient ethanol production from brown macroalgae sugars by a synthetic yeast platform. *Nature* 505, 239–243.
- Gardner, P.R., Fridovich, I., 1991. Superoxide sensitivity of the *Escherichia coli* aconitase. *J. Biol. Chem.* 266, 19328–19333.
- Gustafsson, L., Larsson, K., Larsson, C., Adler, L., 1993. Maintenance energy requirements under stress conditions *Pure & Appl. Chem.* 65, 1893–1898.
- Heavner, B.D., Smallbone, K., Barker, B., Mendes, P., Walker, L.P., 2012. Yeast 5-an expanded reconstruction of the *Saccharomyces cerevisiae* metabolic network. *BMC Syst. Biol.* 6, 55.
- Hjersted, J.L., Henson, M.A., Mahadevan, R., 2007. Genome-scale analysis of *Saccharomyces cerevisiae* metabolism and ethanol production in fed-batch culture. *Biotechnol. Bioeng.* 97, 1190–1204.
- Jang, Y.S., Park, J.M., Choi, S., Choi, Y.J., Seung, D.Y., Cho, J.H., Lee, S.Y., 2012. Engineering of microorganisms for the production of biofuels and perspectives based on systems metabolic engineering approaches. *Biotechnol. Adv.* 30, 989–1000.
- Jung, K.A., Lim, S.R., Kim, Y., Park, J.M., 2013. Potentials of macroalgae as feedstocks for biorefinery. *Bioresour. Technol.* 135, 182–190.
- King, Z.A., Feist, A.M., 2013. Optimizing cofactor specificity of oxidoreductase enzymes for the generation of microbial production strains—OptSwap. *Ind. Biotechnol.* 9, 236–246.
- Llaneras, F., Pico, J., 2008. Stoichiometric modelling of cell metabolism. *J. Biosci. Bioeng.* 105, 1–11.
- Maxwell, W.A., Edward, S., 1971. Mannitol uptake by *Saccharomyces cerevisiae*. *J. Bacteriol.* 105 (3), 753–758.
- Mo, M.L., Palsson, B.Ø., Herrgård, M.J., 2009. Connecting extracellular metabolomic measurements to intracellular flux states in yeast. *BMC Syst. Biol.* 3, 37.
- Nissen, T.L., Ulrik, S., Nielsen, J., Villadsen, J., 1997. Flux distributions in anaerobic, glucose-limited continuous cultures of *Saccharomyces cerevisiae*. *Microbiology* 143, 203–218.
- Orth, J.D., Thiele, I., Palsson, B.Ø., 2010. What is flux balance analysis? *Nat. Biotechnol.* 28, 245–248.
- Overkamp, K.M., Kötter, P., van der Hoek, R., Schoondermark-Stolk, S., Luttik, M.A.H., van Dijken, J.P., Pronk, J.T., 2002. Functional analysis of structural genes for NAD(+)–dependent formate dehydrogenase in *Saccharomyces cerevisiae*. *Yeast* 19, 509–520.
- Quain, D.E., Boulton, B., 1987. Growth and Metabolism of Mannitol by Strains of *Saccharomyces cerevisiae*. *J. Gen. Microbiol.* 133 (7), 1675–1684.
- Rehm, B.H.A. (Ed.), 2009. *Alginates: Biology and Applications*. Springer, Berlin, Heidelberg.
- Savinell, J.M., Palsson, B.Ø., 1992. Network analysis of intermediary metabolism using linear optimization. I. Development of mathematical formalism. *J. Theor. Biol.* 154, 421–454.
- Schellenberger, J., Que, R., Fleming, R.M.T., Thiele, I., Orth, J.D., Feist, A.M., Zielinski, D.C., Bordbar, A., Lewis, N.E., Rahmadian, S., Kang, J., Hyduke, D.R., Palsson, B.Ø., 2011. Quantitative prediction of cellular metabolism with constraint-based models: the COBRA Toolbox v2.0. *Nat. Protoc.* 6, 1290–1307.
- Schulze, U., 1995. *Anaerobic Physiology of Saccharomyces cerevisiae*. Technical University of Denmark.
- Vargas, F., Pizarro, F., Pérez-Correa, J.R., Agosin, E., 2011. Expanding a dynamic flux balance model of yeast fermentation to genome-scale. *BMC Syst. Biol.* 5 (75).
- Varma, A., Palsson, B.Ø., 1994. Metabolic flux balancing: basic concepts, scientific and practical use. *Nat. Biotechnol.* 12, 994–998.
- Visser, W., Scheffers, W.A., Batenburg-van der Vegte, W.H., van Dijken, J.P., 1990. Oxygen requirements of yeasts. *Appl. Environ. Microbiol.* 56, 3785–3792.
- Wargacki, A.J., Leonard, E., Win, M.N., Regitsky, D.D., Santos, C.N.S., Kim, P.B., Cooper, S.R., Raisner, R.M., Herman, A., Sivitz, A.B., Lakshmanaswamy, A., Kashiyama, Y., Baker, D., Yoshikuni, Y., 2012. An engineered microbial platform for direct biofuel production from brown macroalgae. *Science* 335, 308–313.
- Weusthuis, R.A., Visser, W., Pronk, J.T., Scheffers, W.A., Van Dijken, J.P., 1994. Effects of oxygen limitation on sugar metabolism in yeasts: a continuous-culture study of the Kluyver effect. *Microbiology* 140, 703–715.